Supplemental information

SUPPLEMENTAL FIGURES

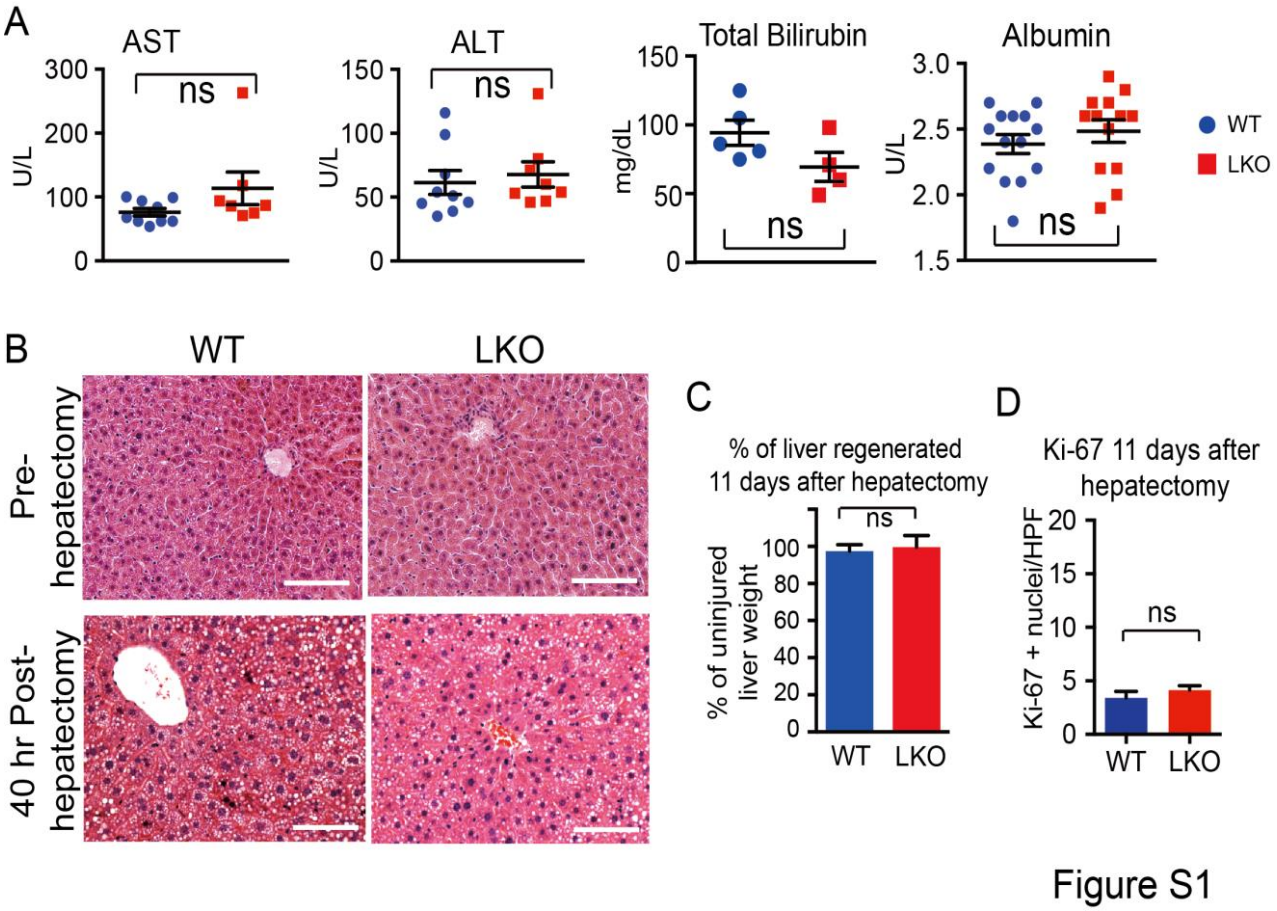

Figure S1

Figure S1. Characterization of *Arid1a* LKO mice during liver regeneration (Related to Figure 1).

(A) Aspartate aminotransferase (AST), Alanine aminotransferase (ALT), Total bilirubin, and Albumin as measured in WT and LKO mice (n is shown in the charts).

(B) Liver histology in *Alb-Cre; Arid1a*$^{Fl/Fl}$ mice at baseline and 40 hours after partial hepatectomy (H+E, Scale bar = 100μm).

(C) % of the original liver mass regenerated in WT and LKO mice 11 days after partial hepatectomy.

(D) Ki-67 IHC quantification in WT and LKO mice 11 days after partial hepatectomy.

All data in this figure are represented as mean +/- SEM, * P<0.05. “n” refers to biological replicates.

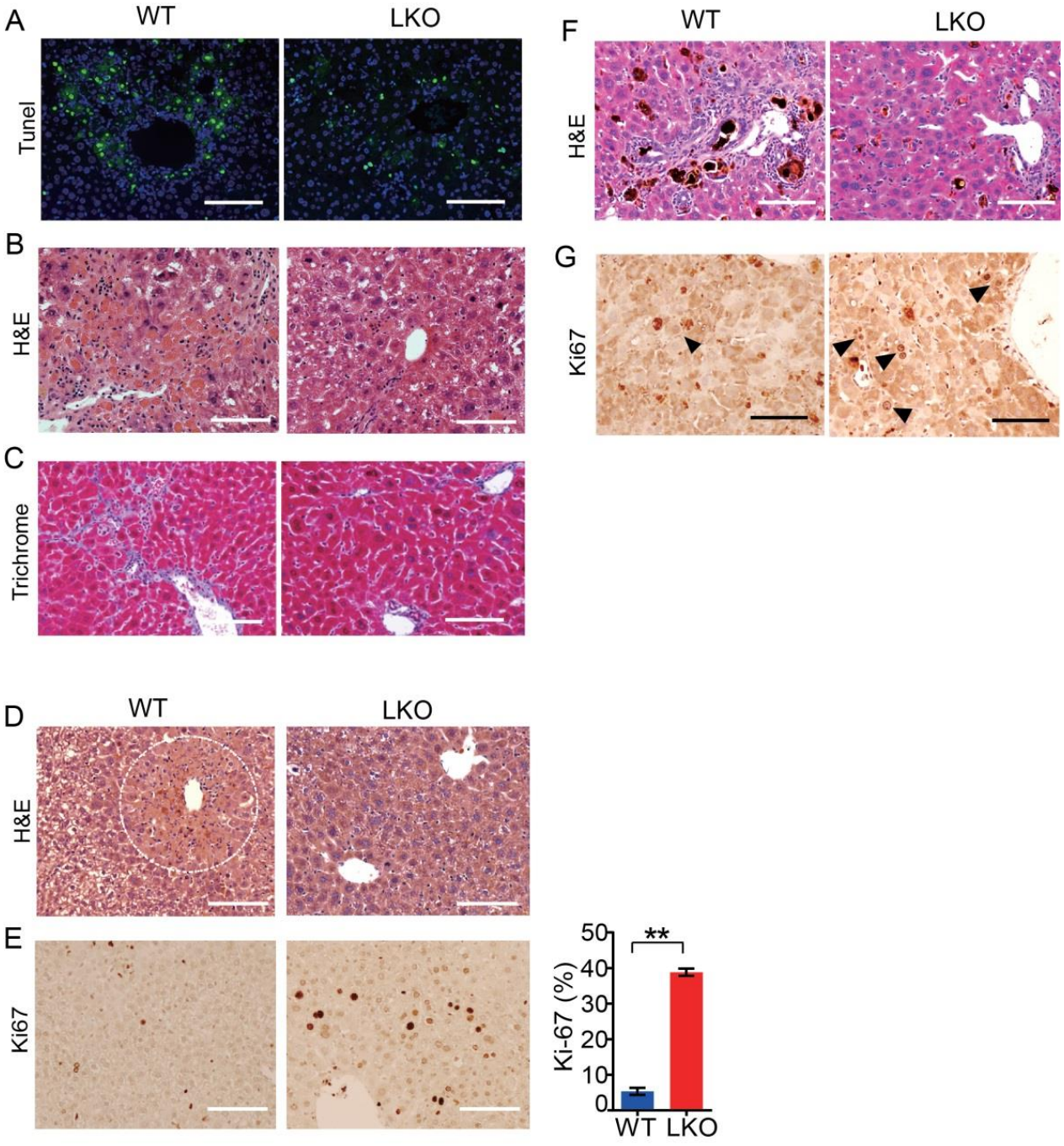
A
WT
LKO
Tunel
B
H&E
C
Trichrome
D
WT
LKO
H&E
E
Ki67
F
WT
LKO
H&E
G
Ki67
**
Ki-67 (%)
50
40
30
20
10
0
WT
LKO

Figure S2

Figure S2. Histological analysis after three chemical injuries (Related to Figure 2).

(A) Apoptosis 24 hours after one CCL4 injection as measured by Tunel staining (Scale bar = 100μm).

(B) WT and LKO liver histology in 5 month-old female mice after 12 weeks of chronic biweekly CCL4 injury with 24 biweekly injections (Scale bar = 50μm).

(C) In mice treated with 12 weeks of chronic biweekly CCl4 injections, fibrosis was detected with trichrome staining (Scale bar = 50μm).

(D) H+E of liver tissue 24 hours after a single IP injection of 300mg/kg of Acetaminophen. Peri-central zonal necrosis is present in the WT but not the LKO livers. Necrosis is seen as areas of darker pink (inside white dotted circle) against the viable hepatocytes that were pale due to steatosis and ballooning injury (Scale bar = 100μm).

(E) Proliferation 24 hours after Acetaminophen injection, as measured by Ki-67 immunostaining. Ki-67 quantification shown on the right (n = 2 and 2 females). Data is represented as mean +/- SEM, * $P<0.05$, ** $P< 0.01$.

(F) H+E (Scale bar = 100μm) and

(G) Ki-67 immunostaining (black arrowheads point to positive nuclei, Scale bar = 100μm) of mouse livers exposed to DDC food for six weeks.

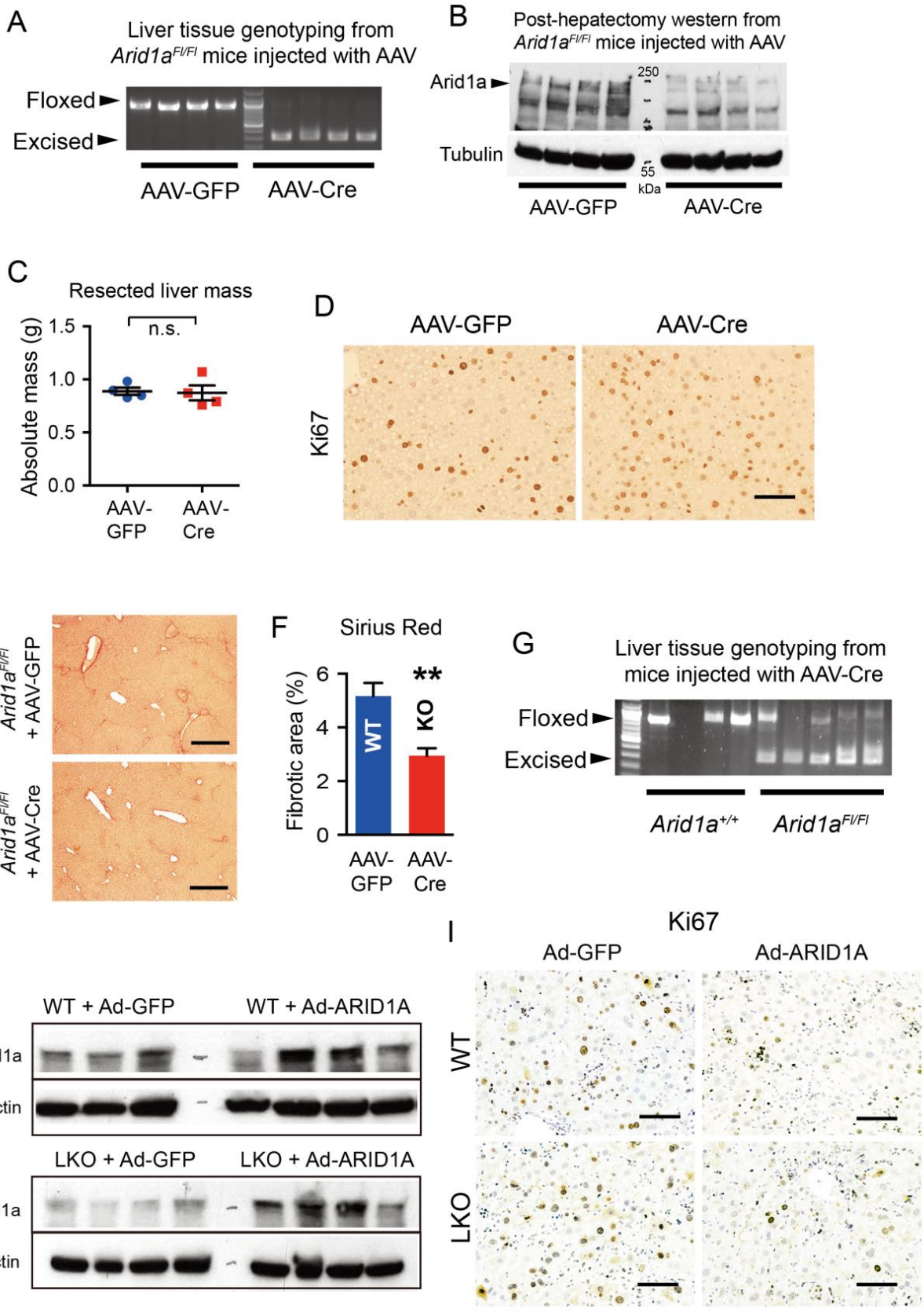
A
Liver tissue genotyping from
Arid1a^Fl/Fl mice injected with AAV
Floxed
Excised
AAV-GFP
AAV-Cre
B
Post-hepatectomy western from
Arid1a^Fl/Fl mice injected with AAV
Arid1a
Tubulin
250
55
kDa
AAV-GFP
AAV-Cre
C
Resected liver mass
n.s.
Absolute mass (g)
1.5
1.0
0.5
0.0
AAV-GFP
AAV-Cre
D
AAV-GFP
AAV-Cre
Ki67
E
Arid1a^Fl/Fl + AAV-GFP
Arid1a^Fl/Fl + AAV-Cre
F
Sirius Red
Fibrotic area (%)
6
4
2
0
**
WT
KO
AAV-GFP
AAV-Cre
G
Liver tissue genotyping from
mice injected with AAV-Cre
Floxed
Excised
Arid1a+/+
Arid1aFl/Fl
H
WT + Ad-GFP
WT + Ad-ARID1A
Arid1a
Actin
LKO + Ad-GFP
LKO + Ad-ARID1A
Arid1a
Actin
I
Ki67
Ad-GFP
Ad-ARID1A
WT
LKO

Figure S3

Figure S3. Data related to Figure 3.

(A) Fourteen days after AAV-GFP or AAV-Cre delivery, we confirmed successful *Arid1a* deletion by genotyping PCR and

(B) protein reduction by western blot analysis.

(C) Resected liver mass during partial hepatectomy (n = 4 and 4).

(D) Hepatocyte proliferation as measured by Ki-67 immunohistochemistry.

(E) *Arid1a*$^{Fl/Fl}$ mice were injected with biweekly CCL4 for 12 weeks. Then CCL4 was stopped and mice were randomized to either 5 x 10^{10} particles of AAV-GFP or AAV-Cre to delete *Arid1a* in hepatocytes only. Livers were examined for fibrosis using Sirius Red after 20 days (n = 6 AAV-GFP and 5 AAV-Cre treated mice, Scale bar = 200μm).

(F) Quantification of Sirius Red staining area (n = 6 AAV-GFP and 5 AAV-Cre mice, 7 HPFs averaged for each mouse).

(G) For DDC experiment, genotyping of *Arid1a*$^{Fl/Fl}$ livers injected with 5 x 10^{10} particles of AAV-GFP or Cre.

(H) Western blot for human ARID1A in WT and *Arid1a* LKO livers treated with Ad-GFP and Ad-ARID1A (n = 3, 4, 4, 4).

(I) Ki-67 immunostaining (Scale bar = 100μm) in these livers 48 hours after one injected dose of CCL4.

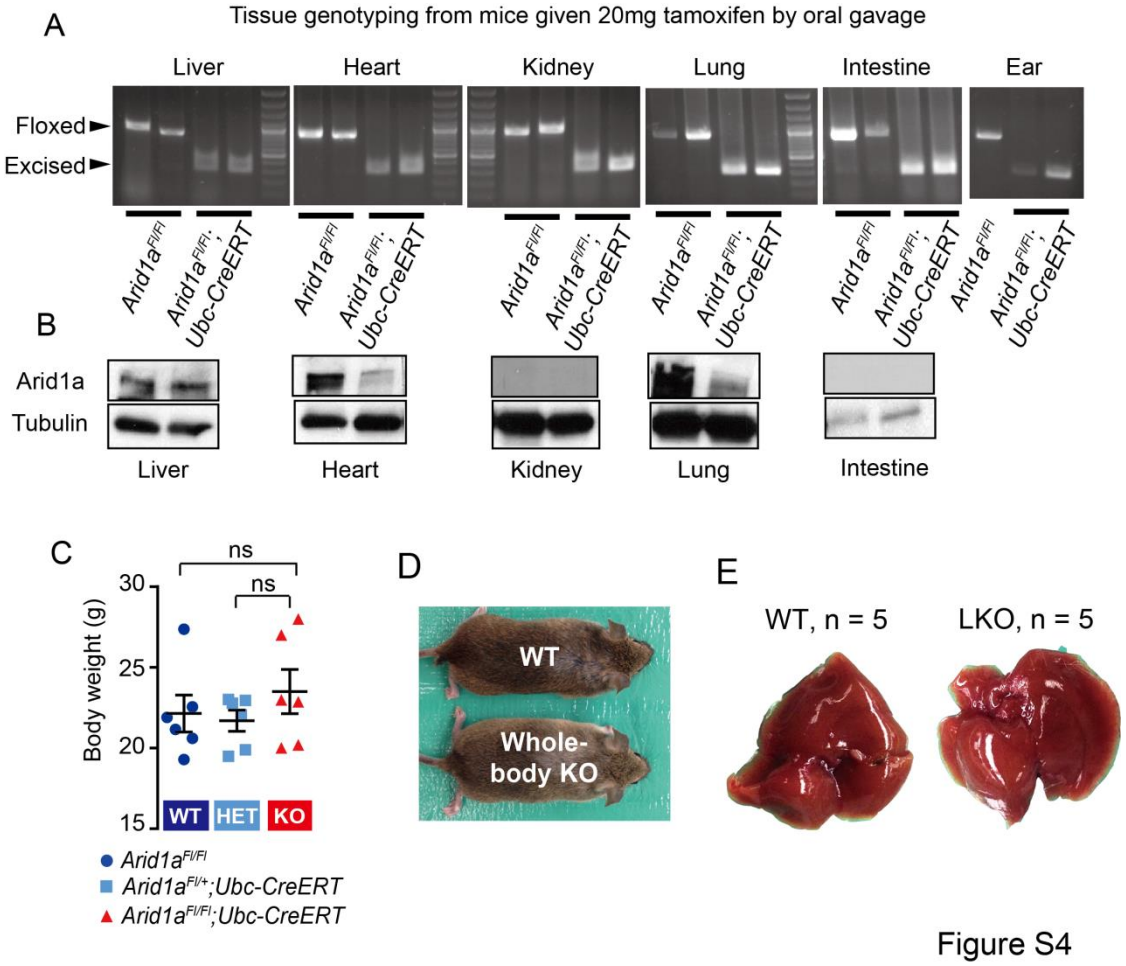

Figure S4

Figure S4. Characterization of whole-body *Arid1a* KO mice (Related to Figure 4).

(A) Genotyping of the *Arid1a* locus in multiple tissues after 20mg tamoxifen delivery by oral gavage. The top band is the floxed band (812 bp), while the lower one is the excised band (268 bp).

(B) Western blot showing Arid1a in various tissues from *Arid1a*$^{Fl/Fl}$ and *Ubc-CreER; Arid1a*$^{Fl/Fl}$ mice injected 500uL of 20mg/mL Tamoxifen for two consecutive days at one month of age.

(C) Body weights of 6 week old *Arid1a*$^{Fl/Fl}$, *Ubiquitin-CreER; Arid1a*$^{+/Fl}$, and *Ubiquitin-CreER; Arid1a*$^{Fl/Fl}$ mice 2 weeks after tamoxifen (n = 6 WT, 4 Het, 3 KO, all males).

(D) 12-month old WT and whole-body *Arid1a* KO mice. At one-month of age, tamoxifen was used to induce *Arid1a* deletion (n = 8 WT and 8 KO).

(E) Representative images of 12-month old WT and LKO livers (n = 5 WT and 5 LKO males). All data in this figure are represented as mean +/- SEM, * P<0.05, ** P< 0.01. “n” refers to biological replicates.

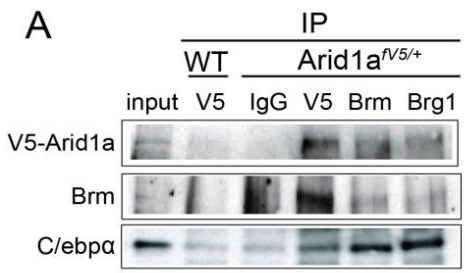
A
IP
WT
Arid1a$^{fV5/+}$
input V5 IgG V5 Brm Brg1
V5-Arid1a
Brm
C/ebpα

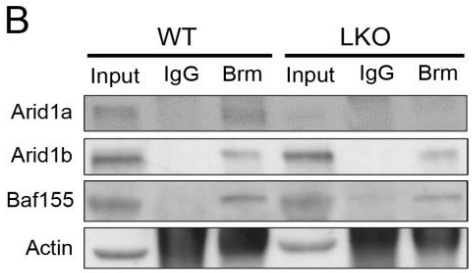
B
WT
LKO
Input IgG Brm Input IgG Brm
Arid1a
Arid1b
Baf155
Actin

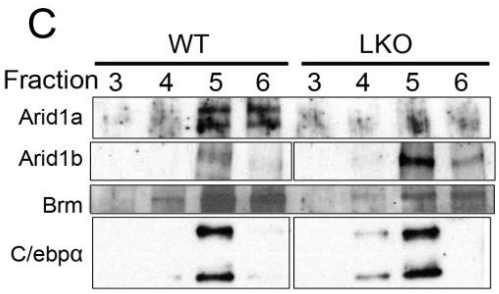
C
WT
LKO
Fraction 3 4 5 6 3 4 5 6
Arid1a
Arid1b
Brm
C/ebpα

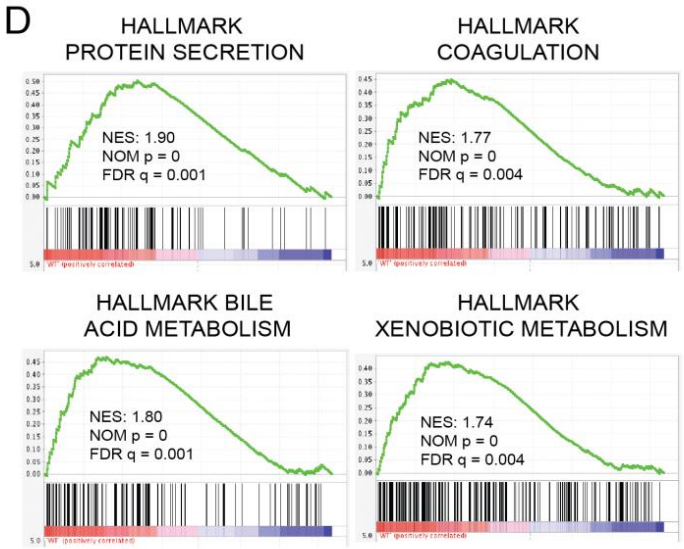
D
HALLMARK PROTEIN SECRETION
NES: 1.90
NOM p = 0
FDR q = 0.001
HALLMARK COAGULATION
NES: 1.77
NOM p = 0
FDR q = 0.004
HALLMARK BILE ACID METABOLISM
NES: 1.80
NOM p = 0
FDR q = 0.001
HALLMARK XENOBIOTIC METABOLISM
NES: 1.74
NOM p = 0
FDR q = 0.004

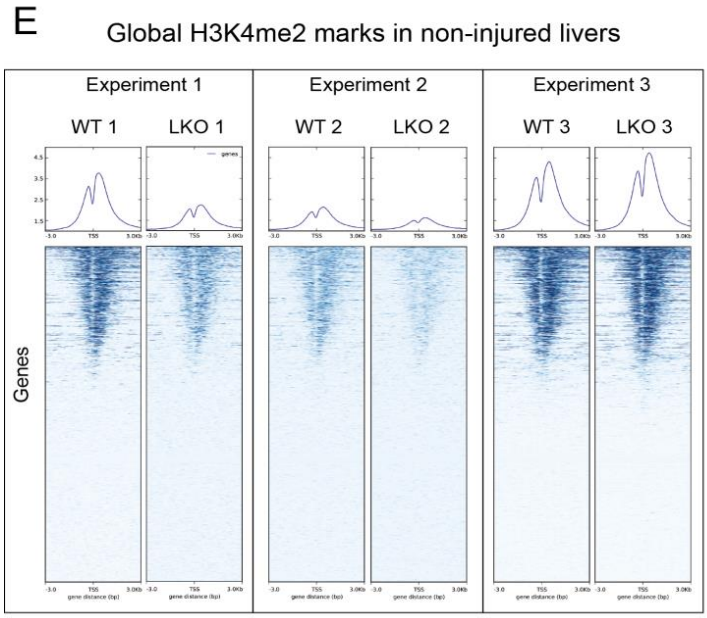
E
Global H3K4me2 marks in non-injured livers
Experiment 1
Experiment 2
Experiment 3
WT 1
LKO 1
WT 2
LKO 2
WT 3
LKO 3
Genes

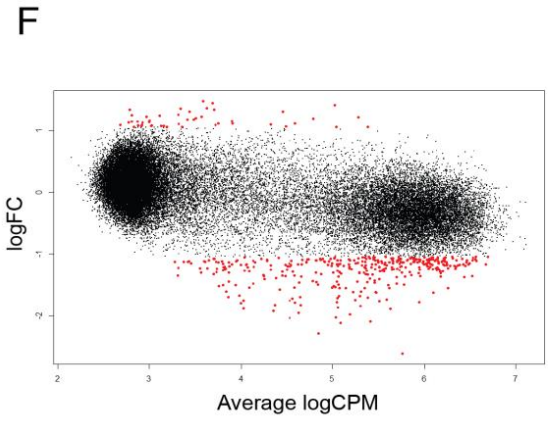
F
logFC
Average logCPM

Figure S5

Figure S5. Data related to Figure 5.

(A) Co-IP experiments between Arid1a, C/ebpα, Brm, and Brg1. A knock-in mouse carrying *Arid1a* fused to a V5 tag (*Arid1a*$^{fV5/+}$ mice) was used to pull down of Arid1a protein with a V5 antibody. V5 antibody was also used in non-transgenic WT livers as an additional negative control. Brm antibodies were used to pull down other SWI/SNF members as well as C/ebpα.

(B) Co-IP with Brm antibody identifies SWI/SNF complex components in either WT or LKO livers.

(C) Size-exclusion chromatography with nuclear lysates from *Arid1a* WT or LKO livers. Eluted fractions were probed with Arid1a, Arid1b, Brm, and C/ebpα antibodies.

(D) GSEA of RNA-seq data reveals that WT livers have increased protein secretion, coagulation, bile acid and xenobiotic metabolism gene signatures. Nominal enrichment score (NES), nominal p-value, and False discovery rate (FDR) q-value are shown in each GSEA plot.

(E) Genome-wide H3K4me2 marks at TSSs. Three independent ChIP-seq experiments were performed for each genotype (n = 3 and 3 WT and LKO mice).

(F) In this plot, each dot represents a gene's TSS region with X and Y-axes representing log counts per million and log fold change values, respectively. Out of 46515 TSS regions, 413 are significantly differentially bound (FDR<0.05) and are highlighted in red. To check for global reduction of signal in LKO compared to WT liver, the Wilcoxon signed rank test was applied to the significant gene regions and the *p*-value is less than 2.2×10^{-16}.

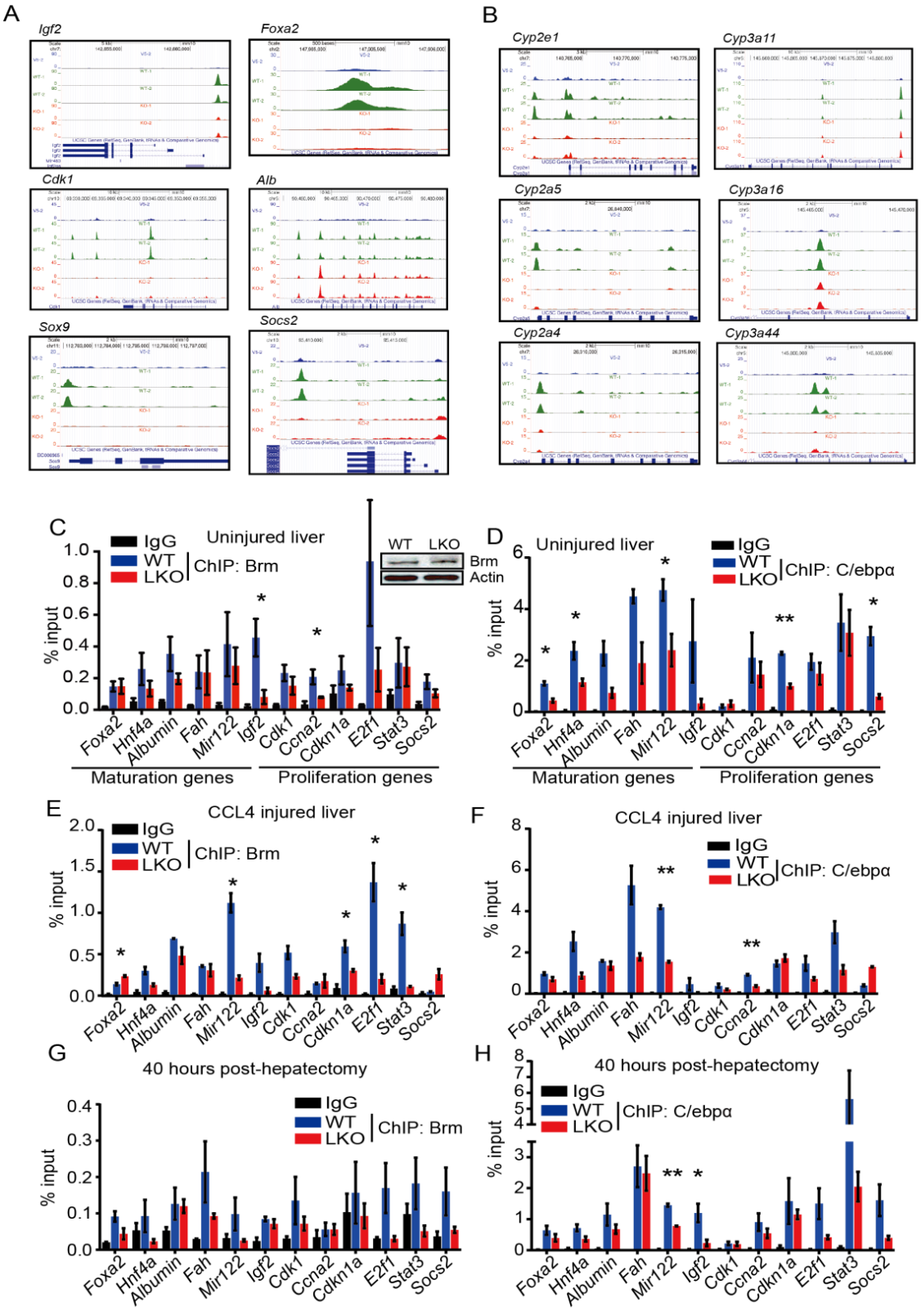
A
Igf2
Foxa2
Cdk1
Alb
Sox9
Socs2
B
Cyp2e1
Cyp3a11
Cyp2a5
Cyp3a16
Cyp2a4
Cyp3a44
C
IgG
WT
LKO
ChIP: Brm
Uninjured liver
WT LKO
Brm
Actin
% input
Foxa2
Hnf4a
Albumin
Fah
Mir122
Igf2
Cdk1
Ccna2
Cdkn1a
E2f1
Stat3
Socs2
Maturation genes
Proliferation genes
D
Uninjured liver
ChIP: C/ebpα
E
CCL4 injured liver
ChIP: Brm
F
CCL4 injured liver
ChIP: C/ebpα
G
40 hours post-hepatectomy
ChIP: Brm
H
40 hours post-hepatectomy
ChIP: C/ebpα

Figure S6

Figure S6. ChIP-seq and ChIP-qPCR data related to Figure 5.

(A) Individual peak traces from ChIP-seq showing common V5-Arid1a targets and C/ebpα targets in the context of uninjured WT and LKO livers. Note that in all of these cases, C/ebpα peaks are quantitatively smaller in the *Arid1a* deficient setting. Two ChIP-seq experiments were performed for each condition except for V5-Arid1a, where one sequencing experiment was performed.

(B) Cytochrome P450 loci commonly bound by V5-Arid1a and C/ebpα are shown.

(C) ChIP-qPCR with IgG and Brm antibody in uninjured WT and LKO livers (n = 4 and 4).

(D) ChIP-qPCR with IgG and C/ebpα antibody in uninjured WT and LKO livers (n = 3 and 3).

(E) ChIP-qPCR with IgG and Brm antibody in WT and LKO livers 6 hours after one CCL4 injection (n = 2 and 2).

(F) ChIP-qPCR with IgG and C/ebpα antibody in WT and LKO livers 6 hours after one CCL4 injection (n = 2 and 2).

(G) ChIP-qPCR with IgG and Brm antibody in WT and LKO livers 40 hours after partial hepatectomy (n = 3 and 3).

(H) ChIP-qPCR with IgG and C/ebpα antibody in WT and LKO livers 40 hours after partial hepatectomy (n = 3 and 3).

All data in this figure are represented as mean +/- SEM, * P<0.05, ** P< 0.01. “n” refers to biological replicates. All ChIP-qPCR experiments were performed five times.

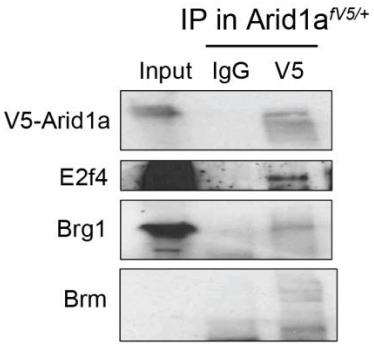

Figure S7

Figure S7. Data related to Figure 6.

Co-IP experiments between V5-Arid1a, E2f4, Brm, and Brg1. These were performed in WT livers.

SUPPLEMENTAL TABLE 1, related to Figure 5 and Figure 6.

(See accompanying Excel files)

Table S1. ChIP-seq data.

Sheet 1. ChIP-seq identified V5-Arid1a bound peaks in *Arid1a*$^{fV5/+}$ livers. All identified peaks ranked by q-value are listed.

Sheet 2. ChIP-seq identified Hnf4a bound peaks in WT p12 livers.

Sheet 3. Common Arid1a and Hnf4a peaks.

Sheet 4. ChIP-seq identified C/ebpα bound peaks in WT livers. Two independent experiments from two livers were performed, and commonly identified peaks are listed.

Sheet 5. Common Arid1a and C/ebpα peaks.

Sheet 6. Peaks differentially bound by C/ebpα in WT and LKO livers. A cutoff of FDR < 0.001 was used to generate this list.

Sheet 7. Peaks within 500bp of TSSs bound by E2f4 in WT and LKO livers 40 hours after partial hepatectomy.

List of Primers used in this study.

Primer	Sequence (5' to 3')	Purpose
mGapdh-F	ACCACAGTCCATGCCATCAC	qPCR
mGapdh-R	TCCACCACCCTGTTGCTGTA	qPCR
m18S-F	CGGCTACCACATCCAAGGAA	qPCR
m18S-R	AGCCGCGGTAATTCCAGC	qPCR
mArid1a-F	TCCCAGCAAACTGCCTATTC	qPCR
mArid1a-R	CATATCTTCTTGCCCTCCCTTAC	qPCR
mActinB-F	CAGAAGGAGATTACTGCTCTGGCT	qPCR
mActinB-R	TACTCCTGCTTGCTGATCCACATC	qPCR
mCcnd1-F	TGCCATCCATGCGGAAA	qPCR
mCcnd1-R	AGCGGGAAGAACTCCTCTTC	qPCR
mCcna2-F	TGAATCACCACATGCTAT	qPCR
mCcna2-R	TAACCTCCATTTCCCTAAG	qPCR
mCcnb1-F	CTCTGTAGTGAATATGTG	qPCR
mCcnb1-R	CATCTGAACCTGTATTAG	qPCR
mCcnb2-F	TCTTGCCTGTCTCAGAAG	qPCR
mCcnb2-R	CTCCATGTAGCCTGTGTAA	qPCR
mCyp1a1-F	GTCCAGCTGTCAGATGATAAGG	qPCR
mCyp1a1-R	TACATGAGGCTCCACGAGATA	qPCR
mCyp2d22-F	TTGAACTACAGGGCTTCCTTATC	qPCR
mCyp2d22-R	TCTCCCAGACAGTCTCATCTT	qPCR
mCyp3a13-F	GCAGGGATTAGGAGAAGGAAAG	qPCR
mCyp3a13-R	GTGGGTTGTTGAGGGAATCA	qPCR
mCyp3a16-F	ACCGCGTGGACTTTATTTATCT	qPCR
mCyp3a16-R	CTGGGCTGTGATCTCGATTT	qPCR
mCyp3a41-F	CCAGAAGAAACTGCAGGAAGA	qPCR
mCyp3a41-R	CCAGGTATTCCATCTCCATCAC	qPCR
mCyp3a44-F	CAGAAGCACCGAGTGGATTT	qPCR
mCyp3a44-R	CTGGACTGTGATCTCCATGTTAG	qPCR
mCyp2e1-F	TGACTGACTGTCTCCTCATAGA	qPCR
mCyp2e1-R	TCGGCCAAAGTCACAGAAATA	qPCR
mCyp2a12-F	GTCAGCTCCACACTACGATATG	qPCR
mCyp2a12-R	GCCAATCACTCGGTCAATCT	qPCR
mCyp2a22-F	TGAGACAGTCAGCTCCTTACTA	qPCR
mCyp2a22-R	GCCAATCACTCGGTCAATCT	qPCR
mCyp2a4-F	CTTCATCGACTCCTTCCTCATC	qPCR
mCyp2a4-R	GTGCCAGCAAAGAAGAGATTTAG	qPCR
mCyp2a5-F	CAACCCAAAGCACTTCCTAGA	qPCR
mCyp2a5-R	CCAGTCCTTCTCCGAAACAATA	qPCR
mCyp2c29-F	CCAATCCTTCACCAACTTCTCA	qPCR
mCyp2c29-R	AGCTTCCTTCACTGCTTCATAC	qPCR
mCyp2c39-F	GAGGAAGCATTCCAATGGTAGA	qPCR
mCyp2c39-R	TGAGTGTGAAGCGCCTAATC	qPCR
mCyp2c50-F	CAGAGACAACAAGCACAACAC	qPCR
mCyp2c50-R	GCCGATCACATGCTCAATTTC	qPCR
mCyp2j5-F	CTGGTGGAAGCCATAAGAGAG	qPCR
mCyp2j5-R	CCAAAGGTGACAGAGCAAATG	qPCR
mCyp3a11-F	ACCACCAGTAGCACACTTTC	qPCR

mCyp3a11-R	CCAGGTATTCCATCTCCATCAC	qPCR
mCyp4a10-F	CCCTGATGGACGCTCTTTAC	qPCR
mCyp4a10-R	GGGTCAAACACCTCTGGATT	qPCR
mCyp4f14-F	TCTGTCTCATCAGCATCTTTGG	qPCR
mCyp4f14-R	CCGCCGAGAAGGGAATAAAT	qPCR
mCyp1a2-F	TCCTGGAGATCTACCGATACAC	qPCR
mCyp1a2-R	TGACCTGCCACTGGTTTATG	qPCR
mFoxa2_F	AGG CAG CGA TTT GCC TCT	ChIP-qPCR
mFoxa2_R	CCA CAA GGC CCA TTA TTG AT	ChIP-qPCR
mHnf4a_F	GGA AGC CAA TAT GCT GTT GC	ChIP-qPCR
mHnf4a_R	CTC ATG GGT GAT GTT TGC AC	ChIP-qPCR
mE2f1_F	GGT TCA CCG AGA ACA GGA AG	ChIP-qPCR
mE2f1_R	ACT TTG ACC AGG ATG GGA TG	ChIP-qPCR
mCcna2_F	AGA AAC AGA AGA TTT GGG CAC T	ChIP-qPCR
mCcna2_R	ACC GAC AGG CTT ATT TTT ACA GA	ChIP-qPCR
mSocs2_F	TGG GTT TTC TAA CCT AAC CAC AA	ChIP-qPCR
mSocs2_R	GTG TCC CAT GAC TTG CCT TT	ChIP-qPCR
mFah_F	TTG GTT GGC TCA GGT TAA GG	ChIP-qPCR
mFah_R	TCC TTT CAT ATC CTG CCT GTG	ChIP-qPCR
mStat3_F	TCT TTG TTT CCC TAG CTT CTG C	ChIP-qPCR
mStat3_R	TGG TAA ACT CGA CGA GAC GAT	ChIP-qPCR
mIgf2_F	TTG AAC AAG GGG GAG TTT GT	ChIP-qPCR
mIgf2_R	GAT CCC CCA ATT CCT AGG TT	ChIP-qPCR
mCdkn1a_F	AGT TCT TGC CCT GGG TCT TT	ChIP-qPCR
mCdkn1a_R	AGC CCC ATA GCC ACA ACT CT	ChIP-qPCR
mMir122a_F	AAC TCC AAA AGG CAG GGT TT	ChIP-qPCR
mMir122a_R	GAG AAC CAA CAA TAT CTG GGA ATC	ChIP-qPCR
mAlb_F	GCA AAC ATA CGC AAG GGA TT	ChIP-qPCR
mAlb_R	TGG GGT TGA TAG GAA AGG TG	ChIP-qPCR
mArid1a GENO-F	GTAATGGGAAAGCGACTACTGGAG	Genotyping
mArid1a GENO-R	TGTTCATTTTTGTGGCGGGAG	Genotyping